

GLOBAL AND LOCAL FLUCTUATIONS OF WINTER AND SUMMER  
SIMULATIONS WITH THE GLAS CLIMATE MODEL

D. M. Straus and J. Shukla

1. INTRODUCTION

Winter and summer simulations have been carried out with an improved version of the GLAS general circulation model. The model used for the simulations is basically that presented by Halem *et al.* (1979). The changes that were made to the model code involved the use of an improved method of computing the boundary layer fluxes, and a more realistic specification of the albedo of snow and ice covered surfaces. (See Shukla *et al.*, 1980). The Winter integration was initialized with data valid for 0Z of 1 January, 1975, and the summer integration was initialized with data valid for 0Z of 15 June, 1979. Both integrations were carried out for 90 days, during which all the boundary conditions were prescribed to vary smoothly. The observed data consists of the NMC twice-daily analyses for the years 1963-1977. Each particular diagnostic quantity was computed from the model data and each of the 15 years of observations in precisely the same way, wherever possible. The reported observational results are averaged over the 15 winters or summers, as appropriate.

2. STATIONARY WAVES IN THE GEOPOTENTIAL HEIGHT FIELD

Results are presented for the stationary (time averaged) component of the geopotential height. Figure 1a shows the observed winter variance around a latitude circle of the stationary geopotential height, summed over wavenumbers 1-4. The term "stationary" refers to a 90-day average commencing on January 1. The corresponding stationary ultra-long planetary wave variance for the winter model<sup>1</sup> simulation is presented in Figure 1b.

The model results show good overall agreement with the observations, with both variances reaching a maximum in the mid-latitude upper troposphere. The model variance is slightly too weak up to the 250 mb level, above which it fails to show the decrease with height apparent in the observations. It is important to note that the stationary variance of this version of the GLAS climate model shown in Figure 1b shows remarkable improvement over the same variance calculated for the previous version of the model, as presented by Straus and Shukla (1981, their Figure 6a).

The observed summer variance of the stationary component of the geopotential height, summed over wavenumbers 1-4, is presented in Figure 1c. The corresponding model variance is shown in Figure 1d. These quantities were computed in the same manner as for the winter season, except that the averaging period was defined to be 90 days starting on June 15. The simulated ultra-long wave variance agrees well with the observations with regard to the location and strength of the three maxima: one in mid-latitudes at about 300 mb, and two in the subtropics, at 850 mb and 200 mb. Discrepancies include the fact that the

<sup>1</sup> The model results presented will be limited to the domain for which observations were available, namely 20°N to 90°N.

simulated mid-latitude variance does not decrease above 300 mb, the slight northward displacement in the model of the subtropical maximum at 850 mb, and the weakness of the simulated subtropical maximum at 200 mb.

### 3. LOW FREQUENCY PLANETARY WAVES

Most of the zonal and time variance of the transient geopotential height field (exclusive of the annual cycle) is contained in low frequency, planetary scale motions. More specifically, we are referring to fluctuations with periods of 7.5 to 90 days and consisting of zonal wavenumbers 1 to 4.

The vertical and meridional structure of the low frequency planetary wave variance (LFPW) observed in winter is shown in Figure 2a<sup>2</sup>. This variance reaches a maximum slightly above the 300 mb level at about 64N, and shows a decrease above this level. The model variance (Figure 2b) has a similar structure, except that the variance increases up to at least 200 mb. In addition, the model variance is somewhat too small throughout the northern hemispheric extratropical domain. As was the case for the stationary planetary waves, this result represents a great improvement over the simulation of the previous version of the model. (See Straus and Shukla (1981), Figure 2a.)

The observed summer LFPW variance is shown in Figure 2c. The structure of the summer variance is quite similar to that in winter, except that the maximum has moved northward. The magnitude of the variance is much less in the summer. The model summer LFPW variance (Figure 2d) has the same overall dependence on latitude and height as observed, but again it does not decrease above 300 mb (as do the observations), and again the model variances are, in general, too small.

### 4. LOCAL ANALYSIS OF VARIANCE

A useful description of the fluctuations of any basic field is afforded by the analysis of local variability discussed by Blackmon (1976). This method portrays the spatially local fluctuations of a particular field by the construction of maps of its RMS deviation in time. The variability due to baroclinic activity is separated by filtering the data with a 'band-pass' filter which retains fluctuations with periods of 2.5 to 6 days. In the application of this method, an estimate of the annual cycle is removed from the data before either the filtering or the computation of the RMS deviation. The band-pass RMS of the geopotential height is closely associated with regions having a high frequency of cyclonic activity, and so indicates the location of the 'storm tracks' (Blackmon, et al., 1977).

A comparison of the observed winter band-pass RMS of geopotential height (Figure 3a) with that of the model (Figure 3b) shows that there is excellent agreement in terms of both the location and strength of the major areas of cyclonic activity in the north central Pacific and western Atlantic. The observed summer band-pass RMS height field (Figure 3c) shows the two oceanic maxima that were present in the winter map. The Atlantic maximum has been

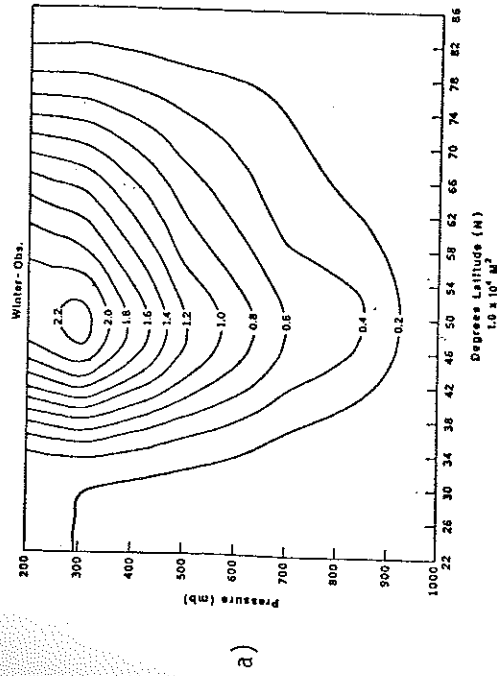
<sup>2</sup> For details regarding the calculation of observed and model LFPW variances, see Straus and Shukla (1981).

shifted to the east, and the magnitude of the summer RMS is generally much smaller. The corresponding map for the model (Figure 3d) indicates that the Atlantic maximum has been realistically simulated, both with respect to position and magnitude. The Pacific maximum, however, is too weak and is located too far to the west.

### REFERENCES

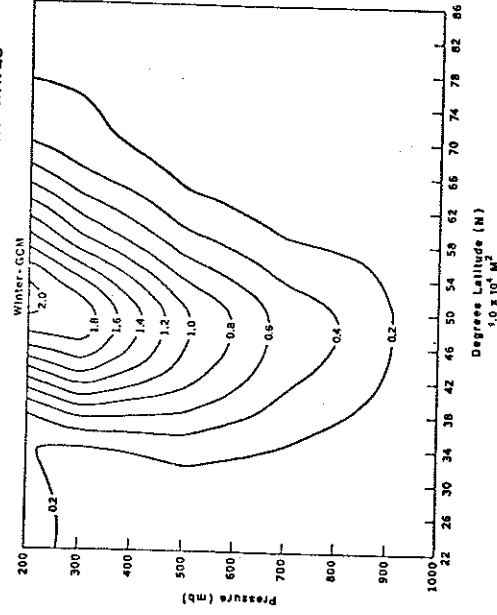
- Blackmon, M. L., 1976: A climatological spectral study of the 500 mb geopotential height of the Northern Hemisphere. J. Atmos. Sci., 33, 1607-1622.
- Blackmon, M. L., J. M. Wallace, N. C. Lau, and S. L. Mullen, 1977: An observational study of the Northern Hemisphere wintertime circulation. J. Atmos. Sci., 34, 1040-1053.
- Halem, M., J. Shukla, Y. Mintz, M. L. Wu, R. Godbole, G. Herman, and Y. Sud, 1979: Comparisons of observed seasonal climate features with a winter and summer numerical simulation produced with the GLAS general circulation model. Report of the JOC Study Conference on Climate Models: Performance, Intercomparison and Sensitivity Studies, Volume I. GARP Publ. Series No. 22, 207-253. WMO, Geneva, Switzerland.
- Lau, N. C., H. Tennekes, and J. M. Wallace, 1978: Maintenance of the momentum flux by transient eddies in the upper troposphere. J. Atmos. Sci., 35, 139-147.
- Shukla, J., Y. Sud, and E. Sabatino, 1980: Preliminary results of a January simulation with an improved version of the GLAS model. Atmospheric and Oceanographic Research Review-1979, NASA Technical Memorandum 80650, pp. 121-132.
- Straus, D. M., and J. Shukla, 1981: Space-time spectral structure of a GLAS general circulation model and a comparison with observations. J. Atmos. Sci., 38, 902-917.

15 YEAR AVERAGE : STATIONARY PLANETARY WAVES



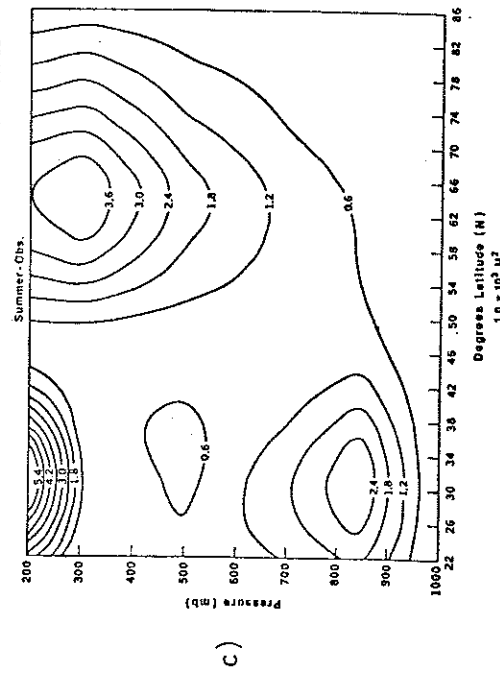
a)

GEOPOTENTIAL STATIONARY PLANETARY WAVES



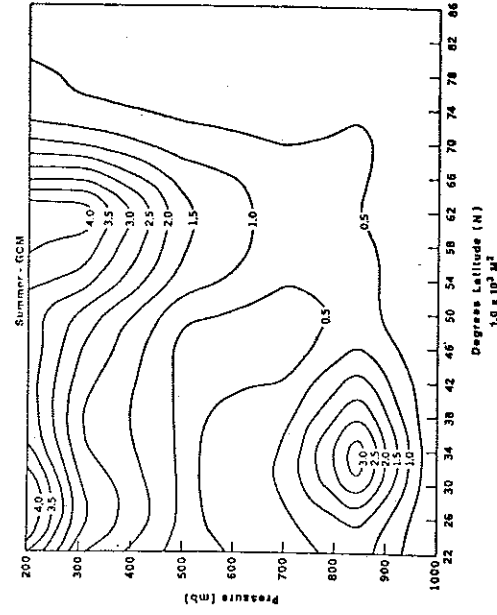
b)

15 YEAR AVERAGE : STATIONARY PLANETARY WAVES



c)

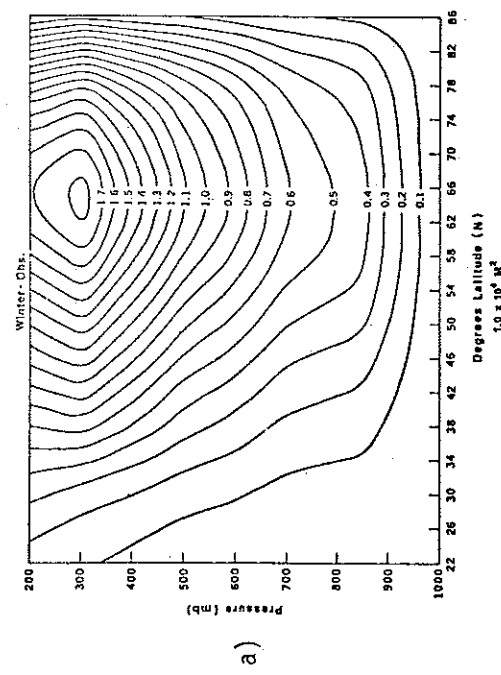
GEOPOTENTIAL STATIONARY PLANETARY WAVES



d)

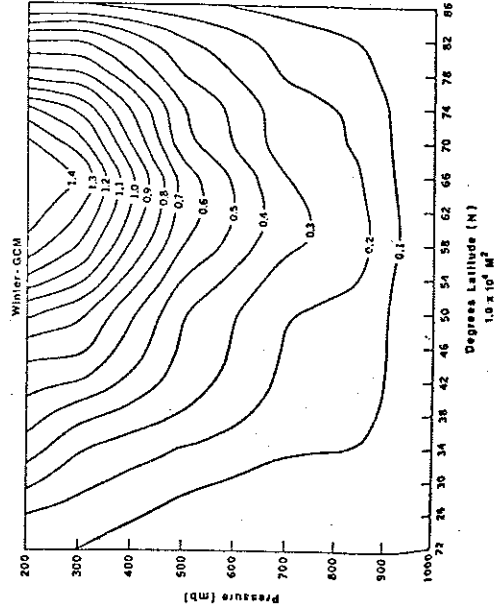
Figure 1. Stationary planetary wave variance of the geopotential height field in the Northern Hemisphere. a) Observations, winter (units of  $10^4 \text{ m}^2$ ); b) Model, winter (units of  $10^4 \text{ m}^2$ ); c) Observations, summer (units of  $10^3 \text{ m}^2$ ); d) Model, summer (units of  $10^3 \text{ m}^2$ ).

15 YEAR AVERAGE : LOW FREQUENCY PLANETARY WAVES



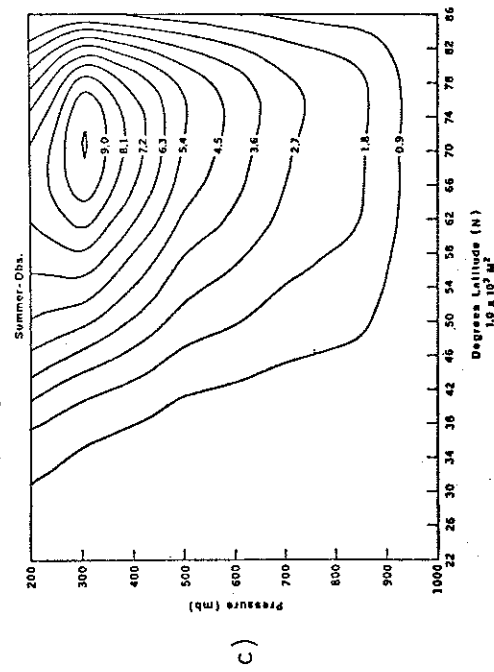
a)

GEOPOTENTIAL HT : LOW FREQUENCY PLANETARY WAVES



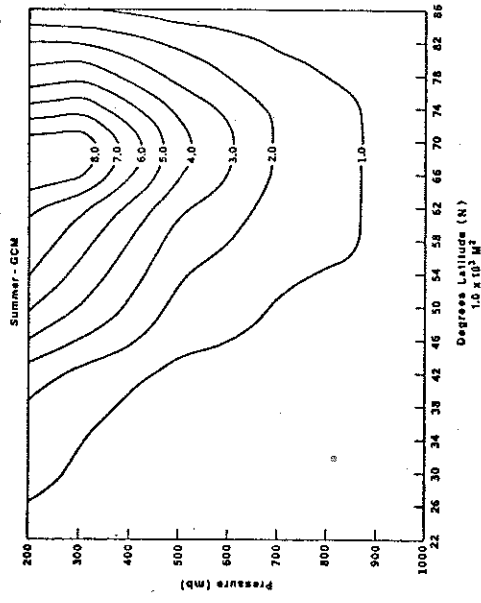
b)

15 YEAR AVERAGE : LOW FREQUENCY PLANETARY WAVES



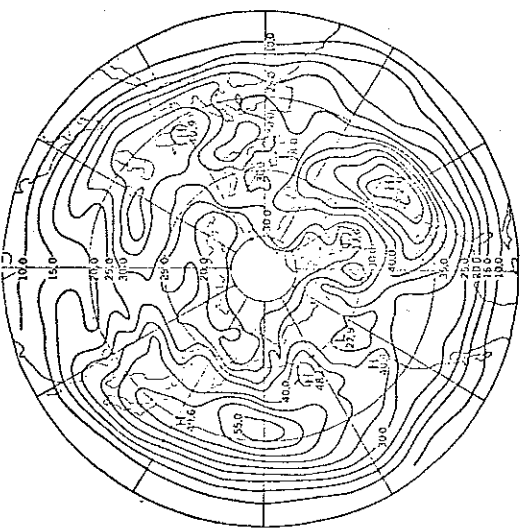
c)

GEOPOTENTIAL HT : LOW FREQUENCY PLANETARY WAVES



d)

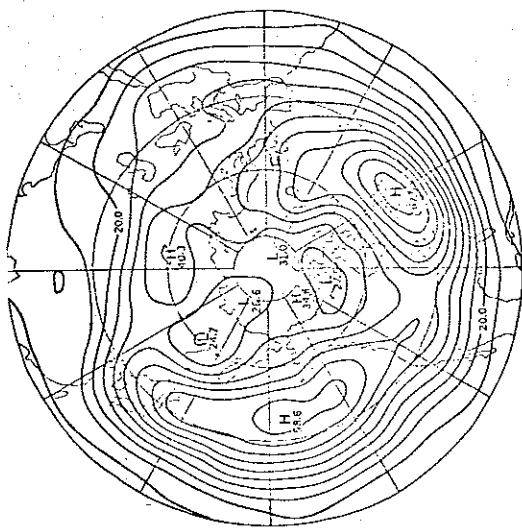
Figure 2. Geopotential height variance in low frequency planetary waves. a) Observations, winter (units of  $10^4 \text{ m}^2$ , contour interval of  $0.1 \times 10^4 \text{ m}^2$ ); b) Model, winter (units of  $10^4 \text{ m}^2$ , contour interval of  $0.1 \times 10^4 \text{ m}^2$ ); c) Observations, summer (units of  $10^3 \text{ m}^2$ , contour interval of  $0.1 \times 10^3 \text{ m}^2$ ); d) Model, summer (units of  $10^3 \text{ m}^2$ , contour interval of  $0.1 \times 10^3 \text{ m}^2$ ).



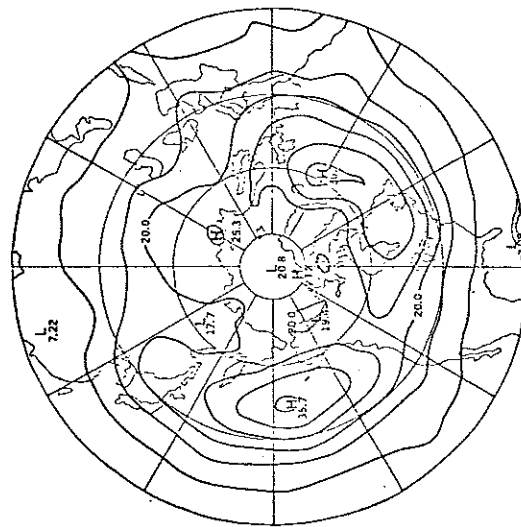
b)



d)



a)



c)

Figure 3. RMS deviation of the 500 mb band-pass geopotential height field, in units of meters. a) Observations, winter (contour interval is 5 m); b) Model, winter (contour interval is 5 m); c) Observations, summer (contour interval is 5 m); d) Model, summer (contour interval is 5 m).